Research Journal of Applied Sciences, Engineering and Technology 8(10): 1174-1190, 2014
DOI:10.19026/rjaset.8.1083
ISSN: 2040-7459; e-ISSN: 2040-7467

Submitted: February 04, 2014 Accepted: March 01, 2014 Published: September 15, 2014

Research Article

Stress-strain Response of High Strength Concrete and Application of the Existing Models

Tehmina Ayub, Nasir Shafiq and M. Fadhil Nuruddin
Department of Civil Engineering, Universiti Teknologi PETRONAS, Bandar Seri Iskandar, Tronoh 31750, Malaysia

Abstract: Stress-strain model of concrete is essentially required during design phases of structural members. With the evolution of normal concrete to High Strength Concrete (HSC); various predictive models of stress-strain behavior of High Strength Concrete (HSC) are available in the literature. Such models developed by various researchers are differing to each other, because of the different mix proportions and material properties. This study represents a comparative analysis of available stress-strain models with the experimental results of three different series (100% cement concrete, Silica Fume (SF) concrete and Metakaolin (MK) concrete) of high strength concrete mixes. Compressive strength and stress-strain behavior of 100×200 mm cylinders made of all Prepared mixes was determined at with curing age of 28 days. Compressive strength of all mixes was found in the range of 71-87 MPa. Stress-strain behavior of tested cylinders was found much different from the available predictive models. In view of the dissimilarity occurred between the predictive stress-strain behavior and the experimental data; a new predictive model is proposed, which adequately satisfy the experimental results.

Keywords: Compressive stress-strain curves, high strength concrete, metakaolin, predictive models, silica fume

INTRODUCTION

Use of High Strength Concrete (HSC) particularly in mega-construction is becoming more popular, because of its value-added benefits, which resulted in the reduction of structural member sizes, durability and longer life. For concrete as structural material, its compressive strength is an essential parameter requires for ultimate strength design of various structural members. Failure response of a structural member is usually studied using nonlinear analysis, for which the compressive stress-strain curves are used as the main design basis (Lu and Zhao, 2010). Recently, Lu and Zhao (2010) represented a review of the compressive stress-strain models published during last few years. It was observed that most of the available models are not capable to predict the stress-strain response of HSC. Therefore, they proposed a new empirical model, which according to them, is found more versatile and applied on all their experimental results and compared with the previously generated stress-strain curves of Hsu and Hsu (1994), Van Gysel and Taerwe (1996) and Wee *et al*. (1996).

An interesting question is to find the reasons of invalidation of predictive models to different sets of experimental results. Undoubtedly, the prediction of concrete behavior has been just like obtaining a specific number by rolling a dice. Where, despite using the same concrete mix ingredients, quantities, size of the molds, curing procedure and temperature, there is less probability of obtaining the same compressive stress-strain behavior and strength. At the time when Popovics (1973) and Carreira and Chu (1985) proposed their models for the compressive strength of HSC, the compressive strength of the concrete was not as high as it is today, even the cement composition has been changed and Superplasticizers (SPs) are so advanced, which can better improve the concrete quality. Therefore, there are very less chances of the potential applicability of the predictive models of Popovics (1973) and Carreira and Chu (1985) for the HSCs of today. Additionally, mineral admixtures or Supplementary Cementitious Materials (SCMs) have now become an essential constituent of the HSC composition, which may possibly influence the stress-strain behavior. Furthermore, the mix design which authors used to propose their predictive models for the compressive stress-strain behavior of HSC were adopted e.g., Popovics (1973), Carreira and Chu (1985), CEB-FIP Model Code 90 (1993), Van Gysel and Taerwe (1996) and Lu and Zhao (2010). Only few researchers used the original mix designs to propose their model e.g., Wang *et al*. (1978), Hsu and Hsu (1994) and Wee *et al*. (1996). Upon reviewing these models, it has been found that, while proposing their models, described the deficiencies of the previous predictive models of the stress-strain behavior of HSC; for example, Hsu and Hsu (1994) claimed that, their model is simple and capable of predicting the complete stress-strain curve of HSC of compressive strength

Corresponding Author: Tehmina Ayub, Department of Civil Engineering, Universiti Teknologi PETRONAS, Bandar Seri Iskandar, Tronoh 31750, Malaysia

Table 1: Existing stress-strain models for HSC

Authors (year)	Model description	Parameter description	Valid compressive strength range (MPa)	Author's remarks
Single model capable of predicting stress-strain response from the origin to ultimate (i.e., $0 < \varepsilon \leq \varepsilon_u$).				
Sargin and Handa (1969)	$\frac{f_c}{f_c'} = k_3 \frac{A\left(\frac{\varepsilon_c}{\varepsilon_c'}\right) + (D-1)\left(\frac{\varepsilon_c}{\varepsilon_c'}\right)^2}{1 + (A-2)\left(\frac{\varepsilon_c}{\varepsilon_c'}\right) + D\left(\frac{\varepsilon_c}{\varepsilon_c'}\right)^2}$	$A = \frac{E_{it}}{E_c}$; $D = 0.65 - 7.25 f_c' \times 10^{-3}$ $E_{it} = 5979\sqrt{f_c'}$; $\varepsilon_c' = 0.0021$	-	
Popovics (1973)	$\frac{f_c}{f_c'} = \frac{\beta\left(\frac{\varepsilon_c}{\varepsilon_c'}\right)}{\beta - 1 + \left(\frac{\varepsilon_c}{\varepsilon_r}\right)^{\beta}}$	$\beta = .058 f_c' + 1$	Up to 51	
Wang *et al*. (1978)	$\frac{f_c}{f_c'} = \frac{A(\varepsilon_c/\varepsilon_c') + B(\varepsilon_c/\varepsilon_c')^2}{1 + C(\varepsilon_c/\varepsilon_c') + D(\varepsilon_c/\varepsilon_c')^2}$	A, B, C and D are constants which can be estimated by considering the condition A $\left\{\frac{f_c}{f_c'} = 0.45 \text{ for } \varepsilon_c/\varepsilon_c' = \frac{0.45}{E_{it}/E_c}\right\}$ $\left\{\frac{f_c}{f_c'} = 1 \quad \text{for} \quad \varepsilon_c/\varepsilon_c' = 1\right\}$	Up to 76	
Carreira and Chu (1985)	$\frac{f_c}{f_c'} = \frac{\beta(\varepsilon_c/\varepsilon_c')}{\beta - 1 + (\varepsilon_c/\varepsilon_c')^{\beta}}$	$\beta = \frac{1}{1 - (\frac{f_c'}{\varepsilon_c' E_{it}})}$ $E_{it} = \frac{f_c'}{\varepsilon_c'}\left(\frac{24.82}{f_c'} + 0.92\right)$ $\varepsilon_c' = (1{,}680 + 7.1\, f_c') \times 10^{-6}$	23 to 80	Does not fit on current data, due to negative value of β
Two models, one for combine prediction of the behavior of rising branch and falling branch up to the limiting strain (i.e., $0 < \varepsilon \leq \varepsilon_{c,lim}$), while the second model predicts the behavior of the depressing branch from limiting strain up to the ultimate strain (i.e., $\varepsilon_{c,lim} < \varepsilon \leq \varepsilon_u$).				
CEB-FIP Model Code 90 (1993)	For $0 \leq \varepsilon \leq \varepsilon_{c,lim}$ $f_c = f_c' \frac{\left(\frac{E_{it}}{E_c}\right)\left(\frac{\varepsilon_c}{\varepsilon_c'}\right) - \left(\frac{\varepsilon_c}{\varepsilon_c'}\right)^2}{1 + \left(\frac{E_{it}}{E_c} - 2\right)\left(\frac{\varepsilon_c}{\varepsilon_c'}\right)}$ For $\varepsilon > \varepsilon_{c,lim}$ $f_c = \frac{f_c'}{\left(\frac{\xi}{\eta_2} - \frac{2}{\eta_2^2}\right)\left(\frac{\varepsilon_c}{\varepsilon_c'}\right)^2 + \left(\frac{4}{\eta_2} - \xi\right)\left(\frac{\varepsilon_c}{\varepsilon_c'}\right)}$	$\frac{\varepsilon_{c,lim}}{\varepsilon_c'} = \frac{1}{2}\left[\left(\frac{E_{it}}{2E_c} + 1\right) + \sqrt{\left(\frac{E_{it}}{2E_c} + 1\right)^2 - 2}\right]$ $\eta_2 = \frac{\varepsilon_{c,lim}}{\varepsilon_c'}$ $\xi = 4\frac{\eta_2^2\left(\frac{E_{it}}{E_c} - 2\right) + 2\eta_2 - \frac{E_{it}}{2E_c}}{\left[\eta_2\left(\frac{E_{it}}{2E_c} - 2\right) + 1\right]^2}$	Up to 90	Modified form of Sargin and Handa (1969)
Hsu and Hsu (1994)	For $0 \leq \varepsilon \leq \varepsilon_{c,lim}$ $\frac{f_c}{f_c'} = \frac{n\beta(\varepsilon_c/\varepsilon_c')}{n\beta - 1 + (\varepsilon_c/\varepsilon_c')^{n\beta}}$ For $\varepsilon > \varepsilon_{c,lim}$ $f_c = 0.3 f_c' e^{-0.8\left(\frac{\varepsilon_c}{\varepsilon_c} - \frac{\varepsilon_{c,lim}}{\varepsilon_c}\right)^{0.5}}$	$\beta = \left(\frac{f_c'}{65.23}\right)^3 + 2.59$ where, $E_{it} = 0.0736 w^{1.51} (f_c')^{0.3}$, $\varepsilon_o = (1680 + 7.1 f_c') \times 10^{-6}$ For $0 \leq \varepsilon \leq \varepsilon_c'$; n=1 For $\varepsilon_c' \leq \varepsilon \leq \varepsilon_d$; n=1 if $f_c' < 62$ MPa n=2 if $62 \text{ MPa} < f_c' < 76$ MPa n=3 if $76 \text{ MPa} < f_c' < 90$ MPa n=5 if $f_c' \geq 90$ MPa $\varepsilon_{c,lim}$ is the strain at $0.3 f_c'$ in the falling branch of stress-strain curve	> 69	The expression is the modified form of Carreira and Chu (1985)
Van Gysel and Taerwe (1996)	For $0 \leq \varepsilon \leq \varepsilon_{c,lim}$ $f_c = f_c' \frac{\left(\frac{E_{it}}{E_c}\right)\left(\frac{\varepsilon_c}{\varepsilon_c'}\right) - \left(\frac{\varepsilon_c}{\varepsilon_c'}\right)^2}{1 + \left(\frac{E_{it}}{E_c} - 2\right)\left(\frac{\varepsilon_c}{\varepsilon_c'}\right)}$ For $\varepsilon > \varepsilon_{c,lim}$ $f_c = \frac{f_c'}{\left(\frac{\xi}{\eta_2} - \frac{2}{\eta_2^2}\right)\left(\frac{\varepsilon_c}{\varepsilon_c'}\right)^2 + \left(\frac{4}{\eta_2} - \xi\right)\left(\frac{\varepsilon_c}{\varepsilon_c'}\right)}$	$\frac{\varepsilon_{c,lim}}{\varepsilon_c'} = \frac{1}{2}\left[\left(\frac{E_{it}}{2E_c} + 1\right) + \sqrt{\left(\frac{E_{it}}{2E_c} + 1\right)^2 - 2}\right]$ $\eta_2 = \frac{\varepsilon_{c,lim}}{\varepsilon_c'}$ $\xi = 4\frac{\eta_2^2\left(\frac{E_{it}}{E_c} - 2\right) + 2\eta_2 - \frac{E_{it}}{2E_c}}{\left[\eta_2\left(\frac{E_{it}}{2E_c} - 2\right) + 1\right]^2}$	Up to 90	The expression is the modified form of CEB-FIP Model Code 90 (1993)
Lu and Zhao (2010)	For $0 \leq \varepsilon \leq \varepsilon_L$ $\frac{f_c}{f_c'} = \left[\frac{(E_{it}/E_c)(\varepsilon_c/\varepsilon_c') - (\varepsilon_c/\varepsilon_c')^2}{1 + (E_{it}/E_c - 2)(\varepsilon_c/\varepsilon_c')}\right]$ For $\varepsilon > \varepsilon_d$ $\frac{f_c}{f_c'} = \frac{1}{1 + \lambda[(\varepsilon_c/\varepsilon_c') - 1/(\varepsilon_L/\varepsilon_c') - 1]^{2(1-\lambda)}}$	$\varepsilon_L = \varepsilon_c'\left[\left(\frac{1}{10}\frac{E_{it}}{E_c} + \frac{4}{5}\right) + \sqrt{\left(\frac{1}{10}\frac{E_{it}}{E_c} + \frac{4}{5}\right)^2 - \frac{4}{5}}\right]$ where, ε_L is the strain at $0.8 f_c'$ in the falling branch of stress-strain curve	50-140	For $0 \leq \varepsilon \leq \varepsilon_L$, modified form of Sargin and Handa (1969) and for $\varepsilon > \varepsilon_L$, model of Van Gysel and Taerwe (1996) is used
Two models, one for predicting the behavior of the rising branch up to the peak point (i.e., $0 < \varepsilon \leq \varepsilon_c'$), while the second model for predicting the behavior of falling branch from the peak point to the ultimate (i.e., $\varepsilon_c' < \varepsilon \leq \varepsilon_u$).				
Wee *et al*. (1996)	For $f_c' \leq 50$ MPa $\frac{f_c}{f_c'} = \frac{\beta(\varepsilon_c/\varepsilon_c')}{\beta - 1 + (\varepsilon_c/\varepsilon_c')^{\beta}}$ For $50 < f_c' \leq 120$ MPa $\frac{f_c}{f_c'} = \frac{k_1\beta(\varepsilon_c/\varepsilon_c')}{k_1\beta - 1 + (\varepsilon_c/\varepsilon_c')^{k_2\beta}}$	$\beta = \frac{1}{1 - (\frac{f_c'}{\varepsilon_c' E_{it}})}$ where, $E_{it} = 10{,}200\,(f_c')^{1/3}$ $k_1 = \left(\frac{50}{f_c'}\right)^{3.0}$; $k_2 = \left(\frac{50}{f_c'}\right)^{1.3}$	50- 120	

f_c': The maximum compressive strength in MPa; ε_c': The corresponding strains; β: The parameter that controls the descending branch; w: The unit weigh of the concrete in kg/m^3

exceeding 69 MPa. However, Carreira and Chu (1985) and in CEB-FIP Model Code 90 (1993), stress-strain models were already proposed for compressive strength exceeding 69 MPa and the model of Carreira and Chu (1985) was simpler. Similarly, the model of CEB-FIP Code 90 (1993) has the assumption of the fixed value of the strain and the steepness of the softening branch, which are not appreciated by the researchers (Lu and Zhao, 2010; Van Gysel and Taerwe, 1996) and therefore, predictive model of CEB-FIP Model Code 90 (1993) is not suitable for HSC. Wee *et al*. (1996) proposed their model for HSC of compressive strength ranging from 50 to 120 MPa. The appreciable fact is that, they carried out a vast experimental investigation, which was not done earlier by any author who proposed their models for the compressive stress-strain curves. In order to determine influence of different mix compositions on the stress-strain behavior of their specimens; they (Wee *et al*., 1996) applied four previously proposed models of Hognestad (1951), Wang *et al*. (1978), Carreira and Chu (1985) and CEB-FIP Model Code 90 (1993) to predict the stress-strain curves and found, the model of Wang *et al*. (1978) has the best fit. In spite of the closeness to the actual stress-strain behavior, Wee *et al*. (1996) and Lu and Zhao (2010) did not appreciate the predictive model proposed by Wang *et al*. (1978) due to its complexity, which is tedious and requires computer aid. Therefore, they (Wee *et al*., 1996) proposed a new predictive model, based on the model of Carreira and Chu (1985) (Table 1).

According to the authors of the current investigation, none of the predictive models, themselves, are not deficient as they were mainly based on the experimental results of the others rather than their original experimental investigation. Therefore, there is a great need of experimental investigation to determine the fitting of all predictive models as represented in Table 1. Upon the examination of these models, it can be observed that, the predictive models of HSC are based mainly on the two parameters required to generate stress-strain curves including maximum compressive strength and its corresponding strains. Moreover, to date, three categories of these models are proposed, as follow:

Type I: Single model capable of predicting stress-strain response from the origin to ultimate (i.e., $0 < \varepsilon \leq \varepsilon_u$).

Type II: Two models, one for predicting the behavior of the rising branch up to the peak point (i.e., $0 < \varepsilon \leq \varepsilon_c'$), while the second model for predicting the behavior of falling branch from the peak point to the ultimate (i.e., $\varepsilon_c' < \varepsilon \leq \varepsilon_u$).

Type III: Two models, one for combine prediction of the behavior of rising branch and falling branch up to the limiting strain (i.e., $0 < \varepsilon \leq \varepsilon_{c,lim}$)., while the second model predicts the behavior of the depressing branch from limiting strain up to the ultimate strain (i.e., $\varepsilon_{c,lim} < \varepsilon \leq \varepsilon_u$).

The principal aim of this study is to investigate the stress-strain behavior as obtained by using different predictive models and to identify their deficiencies as highlighted by different researchers. A predictive model is also proposed based on the proposed models of Hsu and Hsu (1994) as well as Lu and Zhao (2010) which is capable of generating stress-strain curves closer to the experimental results.

EXPERIMENTAL PROGRAM

Material properties and mix design: Detail of the material used for the preparation of the HSC and their quantities are presented in Table 2; however, physical and chemical given of cement and mineral admixtures used are listed in Table 3.

Casting and testing of specimens: For each series (Table 2), two batches of HSC were prepared and from each batch, three cylinders of size 100×200 mm were cast and cured for 28 days. Before pouring the concrete in the molds conforming to specification C470/C470M, slump of the concrete was determined, immediately after mixing the concrete in compliance with ASTM C192/C192M-13a and it was found that, slump is within the limit of 100±10 mm then, the all concrete specimens were demolded and cured.

After completion of the curing period, all 12 cylinders (4 cylinders for each series) were tested using compression testing machine of 1000 kN capacity. Before testing, specimens were air dried for a few hours and capped with mortar plaster to ensure the uniform distribution of the compressive load between cylinders and machine. The compression test was performed according to ASTM C39-03 (ASTM, 2003). Strain measurements were recorded using LVDT. The compressive strength results of the best two of three cylinders along with the strain results are given in Table 4. The stress-strain curves for all three series

Table 2: Mix materials and quantities for HSC preparation

	Mix quantity (kg/m^3)							
					Coarse aggregates			
Series	OPC	Silica fume	Metakaolin	Fine aggregate	<10 mm	10-20 mm	Water	Superplasticizer
"P"	450	-	-	670	600	500	180	Variable, target
"S"	405	45	-	670	600	500	180	Slump 100±10 mm
"M"	405	-	45	670	600	500	180	

Table 3: Physical and chemical composition of OPC, SF and MK

	OPC	Silica fume	Metakaolin
Specific gravity	3.050	-	-
BET surface area (m^2/g)	0.392	16.455	12.174
Loss on Ignition (LOI)	-	2.000	1.850
Average particle size (μm)	-	-	2.500-4.500
SiO_2 (%)	20.440	91.400	53.870
Al_2O_3 (%)	2.840	0.090	38.570
CaO (%)	67.730	0.930	0.040
MgO (%)	1.430	0.780	0.960
SO_3 (%)	2.200	-	-
Na_2O (%)	0.020	0.390	0.040
K_2O (%)	0.260	2.410	2.680
TiO_2 (%)	0.170	-	-
MnO (%)	0.160	0.050	0.010
Fe_2O_3 (%)	4.640	-	1.400
TiO_2 (%)	-	0.040	0.950
P_2O_5 (%)	-	0.380	0.100

Properties were determined by X-Ray Fluorescence (XRF) and Brunauer-Emmett-Teller (BET) specific surface area analysis

Table 4: Compression test results at curing age of 28 days

	Actual results					Avg. results (MPa)			
			Strain (mm/mm)						
Series	Cylinder IDs	Compressive strength (MPa)	Peak	Ultimate	Elastic modulus (MPa)	Compressive strength	Elastic modulus	S.D. (MPa)	Sample variance (%)
"P"	Cylinder 1	71.56	0.002309	0.011739	42,347	72.880	42,604	1.750	3.048
	Cylinder 2	72.17	0.002377	0.018320	42,467				
	Cylinder 3	75.45	0.002362	0.012199	43,101				
	Cylinder 4	72.34	0.002204	0.011287	42,500				
"S"	Cylinder 1	82.33	0.002319	0.014198	44,373	79.196	43,944	1.703	2.898
	Cylinder 2	77.24	0.002269	0.017283	43,439				
	Cylinder 3	80.34	0.002305	0.020203	44,013				
	Cylinder 4	80.01	0.002376	0.022226	43,952				
"M"	Cylinder 1	85.23	0.002381	0.011832	44,888	85.750	44,979	1.087	1.182
	Cylinder 2	84.47	0.002416	0.017960	44,754				
	Cylinder 3	86.67	0.002345	0.012493	45,139				
	Cylinder 4	86.64	0.002233	0.013233	45,134				

Avg.: Average; S.D.: Standard deviation

obtained from the testing of 100×200 mm cylinders are shown in Fig. 1.

ANALYSIS OF THE EXPERIMENTAL RESULTS

Compressive strength results consisting of mean strength, standard deviation and sample variance are listed in Table 4. Based on the statistical analysis of the test results, standard deviation was obtained between 1 to 1.75 MPa and the coefficient of variation was found lower than 3%. The consistency of the stress-strain curves is shown in Fig. 1 indicates that, all mixes were well designed and highly cohesive. Highest average compressive strength was obtained in series "M" (Table 4), which was 17.66 and 7.22% higher than series "P" and series "S", respectively. The compressive strength of series "S" was 9.74% higher than of series "P".

Comparison of the mix design used in current investigation: The authors collected the data of the experimental mix designs used to formulate the predictive models for High Strength Concrete (HSC) from 1990 to date to observe the effect of mix design and aggregate size on the stress-strain curves. The experimental investigation carried by the Wee *et al*. (1996) was the only comprehensive and close to the current experimental investigation; however, in rest of the investigations, previously generated data was used. It was however, mentioned by Popovics (1973) and Carreira and Chu (1985) that, there are several unseen factors which affect the stress-strain behavior. For example stress-strain curve is very much sensitive to the testing conditions (type and stiffness of the compression testing machine, loading rate and duration); specimen's shape and size; position, type and length of the strain gages applied on the specimens, specimen age, concrete mix composition (particularly coarse aggregate size and quantity), etc., (Popovics, 1973; Carreira and Chu, 1985). Carreira and Chu (1985) further added that, the shape of the descending branch is influenced by the stiffness of the specimen versus stiffness of the compression testing machine, development of the micro cracks at the interface of the aggregate and cement matrix. That is the reason; stress-strain relation is strongly affected by the rate of the strains, quality, content and characteristics of the cement matrix and aggregates.

Therefore, it is necessary to carry out a comprehensive experimental work while proposing any predictive model so that researchers can better understand the effects of the mentioned

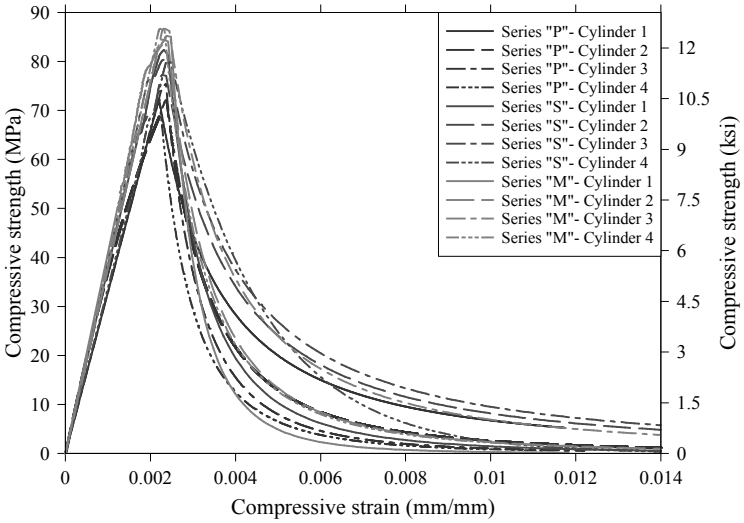

Fig. 1: Experimental stress-strain curves of all investigated series of HSC

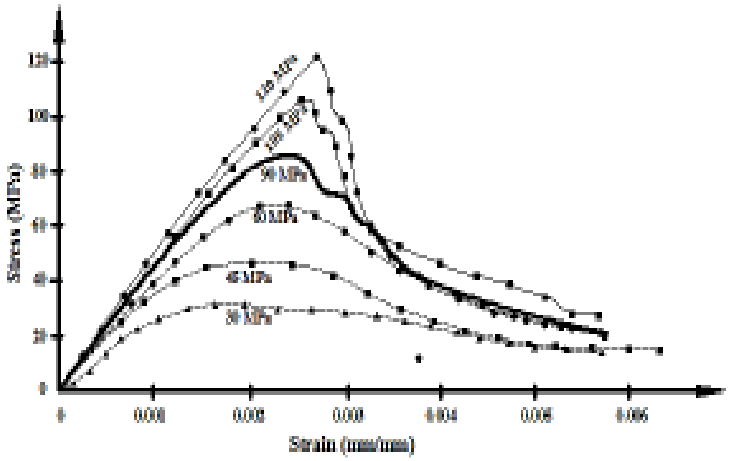

(a)

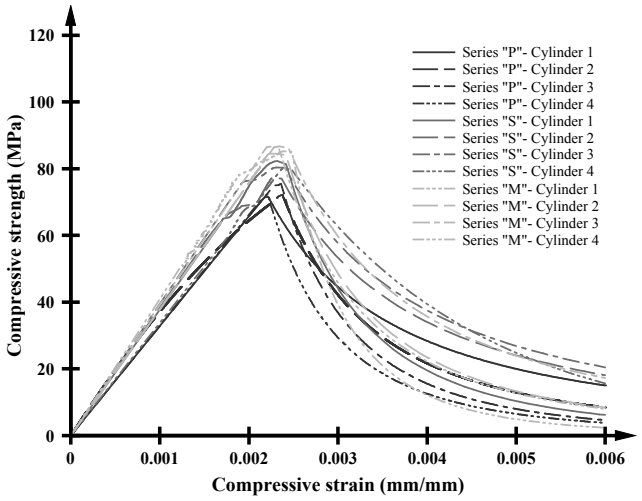

(b)

Fig. 2: Comparison of the current experimental results with the test results of Wee *et al*. (1996)

Table 5: Mix composition and content of FRC used in existing studies

		Mixing materials and their quantities (kg/m^3)									
	Cylinder size				Coarse aggregate						
Authors	(dia.×height) (mm)	Cement	SF (%)	Fine aggregate	Max. size (mm)	Quantity	Water (w/b) ratio	Superplasticizer	Compressive strength (MPa)	Peak strains (mm/mm)	Elastic modulus (GPa)
Wee	100×200	425	-	722	19	1083	170 (0.40)	-	63.2	0.002169	41.8
et al. (1996)		383	42 (10)	722		1083	170 (0.40)		70.2	0.002100	43.0
		437	48 (10)	698		1046	170 (0.35)		85.9	0.002260	45.0
		389	97 (20)	698		1046	170 (0.35)		90.2	0.002430	44.4
		550	-	640		1045	165 (0.30)		78.3	0.002320	44.3
		495	55 (10)	640		1045	165 (0.30)		85.9	0.002310	44.3
		640	-	587		1043	160 (0.25)		85.6	0.002320	45.6
		608	32	587		1043	160 (0.25)		96.2	0.002370	46.6
		576	64	587		1043	160 (0.25)		102.8	0.002470	46.7
		544	96	587		1043	160 (0.25)		104.2	0.002490	46.3
		675	67.5	520		1010	150 (0.20)		119.9	0.002750	49.1

Max.: Maximum

parameters. Though, these parameters are not considered in any of the proposed models (Table 1), but indirectly, few researchers considered material parameter, stress-strain curve shape parameter and/or constants.

The experimental data of Wee *et al*. (1996) is given in Table 5 and compared with the experimental data in Fig. 2.

As mentioned in Table 5, for the same quantity of water and the same size of aggregates, Wee *et al*. (1996) varied their experimental data by increasing the amount of cement paste (cement+water) and lowering of the aggregate content especially fine aggregate. By doing so, higher strength of the concrete was obtained while the post peak branch of the stress strain curve was observed steeper. The increase in compressive strength is mainly due to the increase in the cement content which offered substantial strength to the cement matrix and shifted the failure towards the aggregates and results higher strength properties. Referring to the Fig. 2, it can be seen that the stress-strain curves of current study appropriately close to those of Wee *et al*. (1996). This shows that, predictive model of Wee *et al*. (1996) can closely predicts the stress-strain behaviour of the current study.

Application of the existing predictive stress-strain models on the current data: All models, as listed in the Table 1, are applied on the current experimental results given in Table 3. The predicted and experimental stress-strain curves are presented in Fig. 3 to 5. It can be seen that, the models of Wee *et al*. (1996) and Lu and Zhao (2010) well represent the post peak branch of the stress-strain curves, while the proposed model of Hsu and Hsu (1994) is suitable for the ascending branch. For all models illustrated in Table 1, goodness of fit of the predicted stress-strain curves to the experimental stress-strain curves of series "P" and series "M" is investigated in terms of Root mean square error "RMS" and absolute fraction of variance "V", following the procedure in Khan *et al*. (2013). These parameters were calculated by selecting the stress values obtained by experiment and calculated from the predictive models at the same level of strain values.

"RMS" and "V" were calculated manually using Eq. (1) and (2), which are described as follow (Table 6):

$$RMS = \sqrt{\frac{\sum|t_i - o_i|^2}{n}} \quad (1)$$

$$V = 1 - \frac{\sum|t_i - o_i|^2}{\sum|o_i|^2} \quad (2)$$

where, "t_i", "o_i" and "n" represent the experimental results (used as target), predicted results (used as output) and number of observations, respectively.

As mentioned in Table 5, the model of Wee *et al*. (1996) and Lu and Zhao (2010) better captured the shape of the descending branch of the current experimental results. However, as mentioned by Lu and Zhao (2010), the drawback of the model of Wee *et al*. (1996) is the discontinuity of the curve at maximum compressive stress. Therefore, the proposed model of Lu and Zhao (2010) is selected as the suitable model for the descending branch and the model of Hsu and Hsu (1994) is selected to predict the rising branch of all stress-strain curves shown in Fig. 3 to 5.

Newly proposed compressive stress-strain curves of HSC: As mentioned in the previous section, the models of the Hsu and Hsu (1994) and Lu and Zhao (2010) are the better representative models of the rising and falling branches of the stress-strain curves, respectively. Therefore, two equations are proposed for the current experimental results. The first equation was proposed for $0 < \varepsilon \leq \varepsilon_{c,lim}$, where $\varepsilon_{c,lim}$ is the strain corresponding to the limiting stress ($f_{c,lim}$) level of $0.96f_c^{'}$ in the falling branch, while second equation was proposed for $f_c > f_{c,lim}$ or $f_c > .96\, f_c^{'}$, whereas, Lu and Zhao (2010) suggested the limiting stress ($f_{c,lim}$) level of 0.96 $f_c^{'}$ is the value of $\varepsilon_{c,lim}$ corresponding to 0.8 $f_c^{'}$ (Table 1). The reason for selecting the limiting stress ($f_{c,lim}$) level of 0.96 $f_c^{'}$ in the falling branch is the appearance of discontinuity when the model was applied to the current experimental data.

The description of the proposed equations by the authors of the current study is as follows:

For $0 < \varepsilon \leq \varepsilon_{c,lim}$:

$$f_c = \frac{n\beta(\varepsilon_c/\varepsilon_c')f_c'}{n\beta - 1 + (\varepsilon_c/\varepsilon_c')^{n\beta}} \quad (3)$$

where,

$$\beta = \left(\frac{f_c'}{65.23}\right)^3 + 2.59 \text{ and } n = 3$$

For $\varepsilon > \varepsilon_{c,lim}$:

$$f_c = \frac{f_{c,lim}}{1+0.1(n-1)[\{(\varepsilon_c/\varepsilon_c')-1\}/\{(\varepsilon_{c,lim}/\varepsilon_c')-1\}]^{\{1+0.1(n-1)\}}} \quad (4)$$

In the following Eq. (1) and (2), the term "n" is the parameter, which contributes in the toughness of the curve, while "β" and exponential function "$1 + 0.1\,(n-1)$" decides the shape of the curve in the

Table 6: "RMS" and "V" of the all predictive models

Series	Cylinder	Parameters	Popovics (1973)	Carreira and Chu (1985)	CEB-FIP Model Code 90 (1993)	Hsu and Hsu (1994)	Van Gysel and Taerwe (1996)	Wee *et al*. (1996)	Lu and Zhao (2010)
"P"	Cylinder 1	RMS	4.9950	4.5910	6.9550	3.9640	6.3750	2.5680	3.1110
		Variance	0.8931	0.9169	0.7224	0.9146	0.7726	0.9777	0.9492
	Cylinder 2	RMS	4.7120	5.3630	4.5290	3.3440	4.6120	11.8020	4.2600
		Variance	0.9509	0.9400	0.9537	0.9704	0.9518	0.7887	0.9600
	Cylinder 3	RMS	9.8850	11.0450	7.5940	6.7220	7.6050	18.2630	8.9770
		Variance	0.8578	0.8345	0.9002	0.9142	0.9005	0.6603	0.8725
	Cylinder 4	RMS	10.0220	11.2310	6.7190	6.8250	6.6130	15.2770	7.1000
		Variance	0.8599	0.8366	0.9162	0.9161	0.9214	0.7383	0.9132
	Series "P"	RMS	7.4040	8.0580	6.4490	5.21375	6.3010	11.9780	5.8620
	Average	Variance	0.8904	0.8820	0.8731	0.9288	0.8866	0.7913	0.9237
"S"	Cylinder 1	RMS	5.9910	6.4340	5.8810	4.0490	6.3730	8.7270	3.7400
		Variance	0.9884	0.9868	0.9889	0.9940	0.9869	0.9761	0.9953
	Cylinder 2	RMS	6.5110	6.1090	9.0160	7.1680	8.2790	2.9810	5.0190
		Variance	0.9809	0.9834	0.9638	0.9735	0.9696	0.9962	0.9882
	Cylinder 3	RMS	8.1020	7.5910	10.4570	8.8880	9.4820	0.8050	6.4780
		Variance	0.9442	0.9518	0.9018	0.9218	0.9199	0.9995	0.9618
	Cylinder 4	RMS	4.9930	4.7390	7.2040	8.0500	6.8670	7.5730	4.5010
		Variance	0.9879	0.9892	0.9750	0.9662	0.9773	0.9737	0.9900
	Series "S"	RMS	6.3993	6.2183	8.1395	7.0388	7.7503	5.0215	4.9345
	Average	Variance	0.9754	0.9778	0.9574	0.9639	0.9634	0.9864	0.9838
"M"	Cylinder 1	RMS	7.3250	7.7850	6.9490	5.1460	7.1570	11.0120	5.7180
		Variance	0.9839	0.9820	0.9865	0.9905	0.9858	0.9653	0.9898
	Cylinder 2	RMS	4.6080	4.8500	4.9180	4.9010	3.9010	6.1200	1.3670
		Variance	0.9876	0.9864	0.9853	0.9841	0.9909	0.9786	0.9988
	Cylinder 3	RMS	8.1040	7.7750	11.0280	9.6530	9.2050	1.1230	6.3230
		Variance	0.9209	0.9287	0.8277	0.8413	0.8839	0.9985	0.9411
	Cylinder 4	RMS	5.5450	5.7500	6.9080	6.4250	4.2850	2.2370	3.1780
		Variance	0.9655	0.9637	0.9320	0.9345	0.9752	0.9936	0.9842
	Series "M"	RMS	RMS	6.3960	6.540	7.4510	6.5310	6.1370	5.1230
	Average	Variance	Variance	0.9645	0.9652	0.9329	0.9376	0.9590	0.9840
Average		RMS	6.7330	6.9390	7.3470	6.2610	6.7300	7.3740	4.9810
		Variance	0.9434	0.9417	0.9211	0.9434	0.9363	0.9205	0.9620

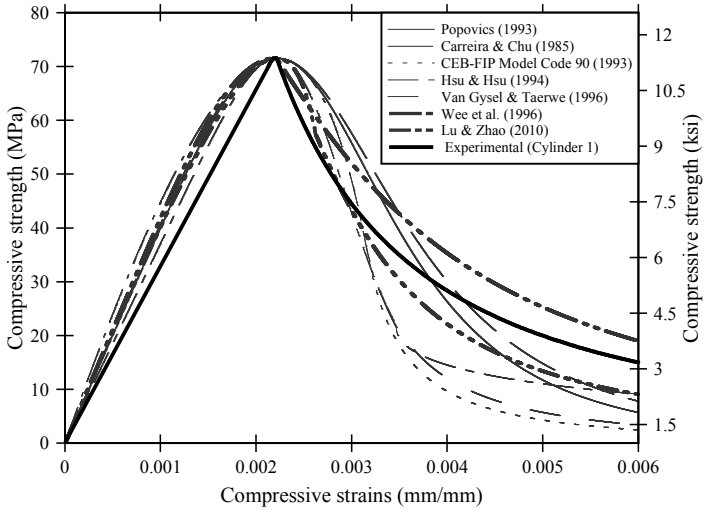

(a)

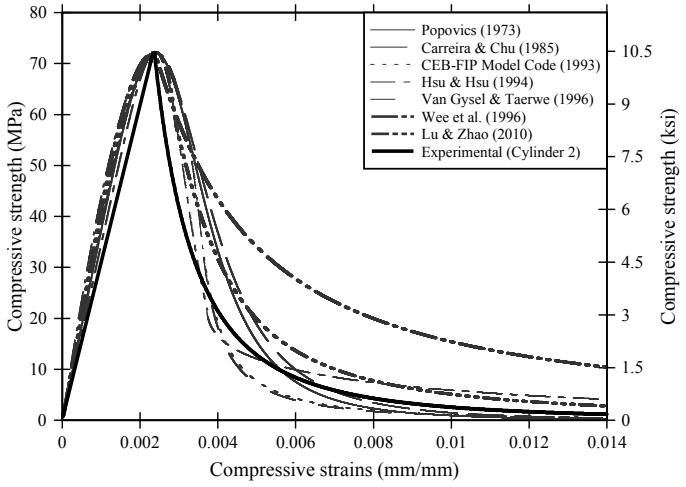

(b)

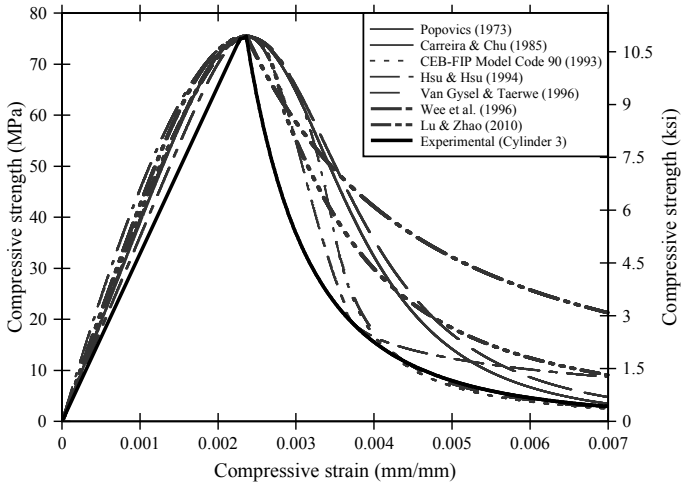

(c)

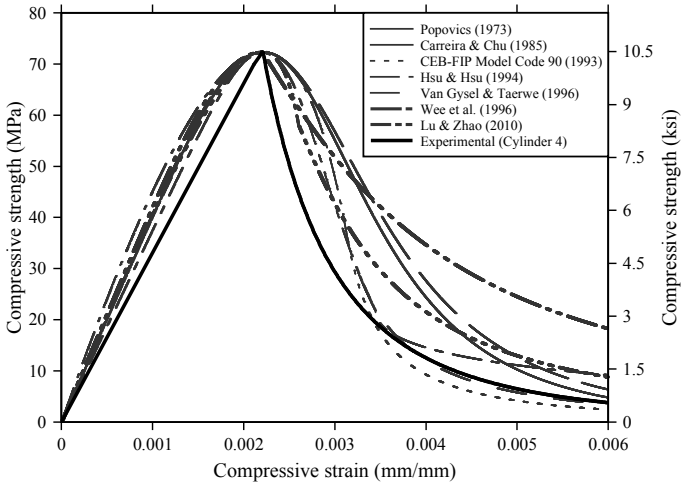

(d)

Fig. 3: Comparison of the predictive and experimental stress-strain curves of series “P"

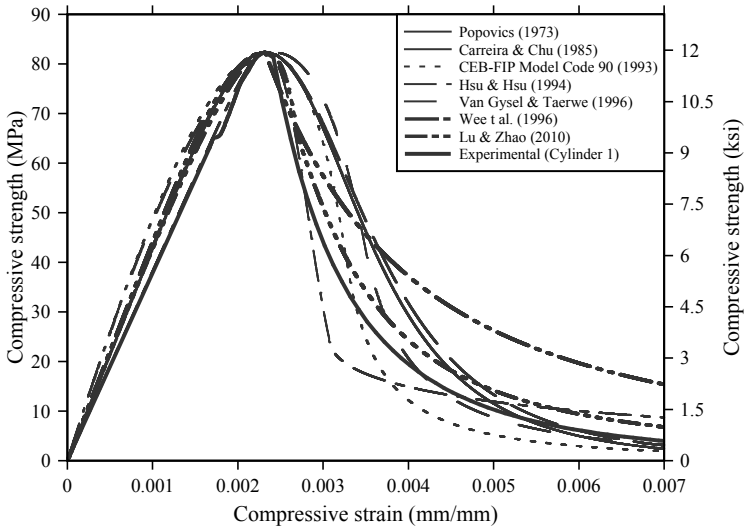
Popovics (1973)
Carreira & Chu (1985)
CEB-FIP Model Code 90 (1993)
Hsu & Hsu (1994)
Van Gysel & Taerwe (1996)
Wee t al. (1996)
Lu & Zhao (2010)
Experimental (Cylinder 1)
Compressive strength (MPa)
Compressive strength (ksi)
Compressive strain (mm/mm)
0
10
20
30
40
50
60
70
80
90
1.5
3
4.5
6
7.5
9
10.5
12
0.001
0.002
0.003
0.004
0.005
0.006
0.007

(a)

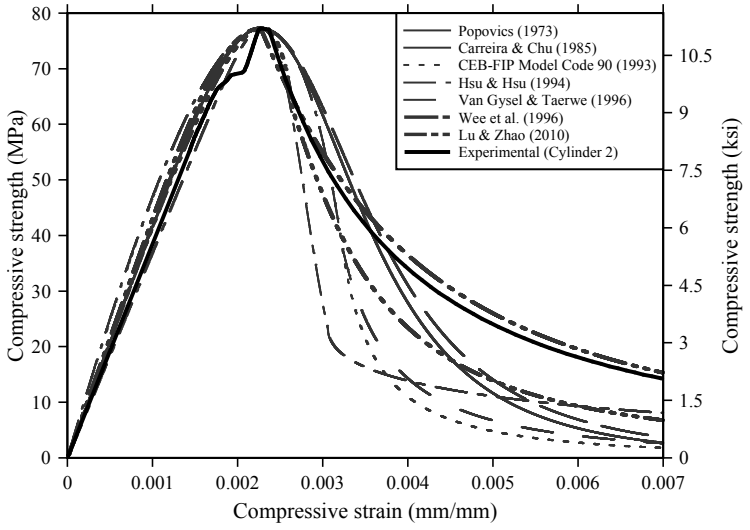
Popovics (1973)
Carreira & Chu (1985)
CEB-FIP Model Code 90 (1993)
Hsu & Hsu (1994)
Van Gysel & Taerwe (1996)
Wee et al. (1996)
Lu & Zhao (2010)
Experimental (Cylinder 2)
Compressive strength (MPa)
Compressive strength (ksi)
Compressive strain (mm/mm)
0
10
20
30
40
50
60
70
80
1.5
3
4.5
6
7.5
9
10.5
0.001
0.002
0.003
0.004
0.005
0.006
0.007

(b)

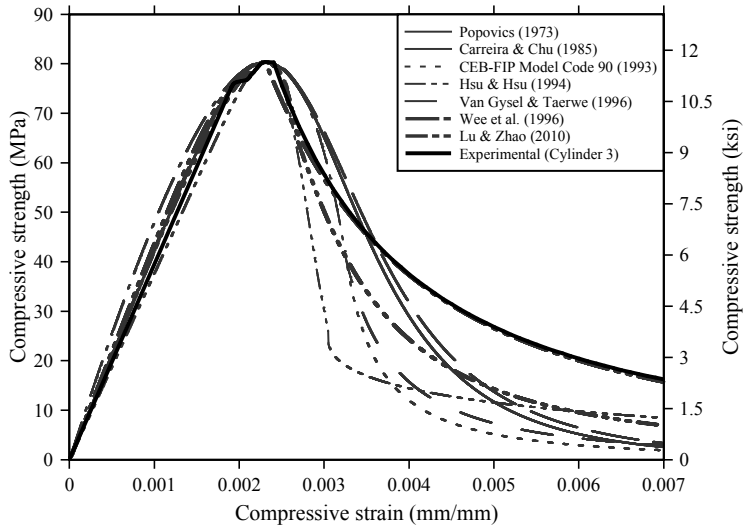
Popovics (1973)
Carreira & Chu (1985)
CEB-FIP Model Code 90 (1993)
Hsu & Hsu (1994)
Van Gysel & Taerwe (1996)
Wee et al. (1996)
Lu & Zhao (2010)
Experimental (Cylinder 3)
Compressive strength (MPa)
Compressive strength (ksi)
Compressive strain (mm/mm)
0
10
20
30
40
50
60
70
80
90
1.5
3
4.5
6
7.5
9
10.5
12
0.001
0.002
0.003
0.004
0.005
0.006
0.007

(c)

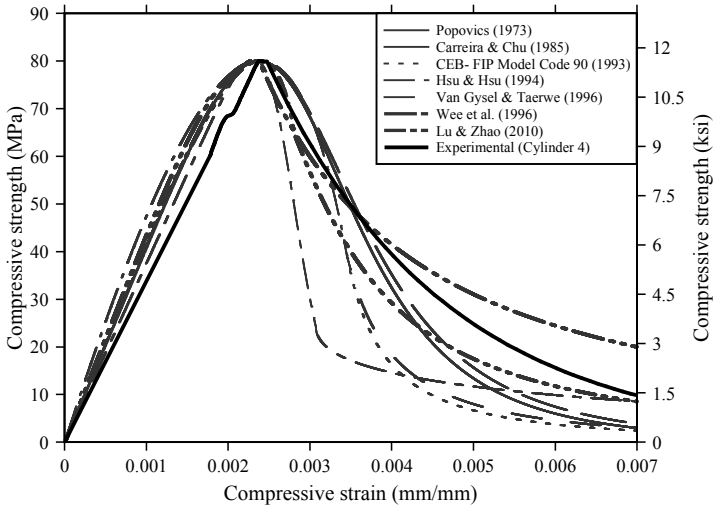

(d)

Fig. 4: Comparison of the predictive and experimental stress-strain curves of series "S"

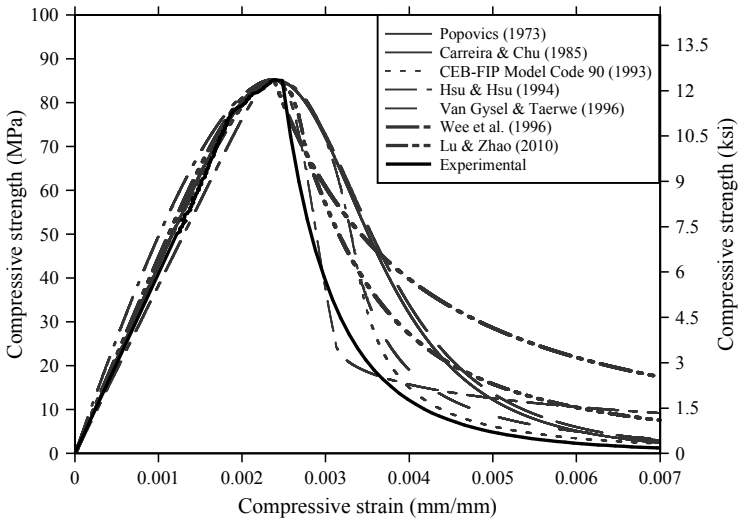

(a)

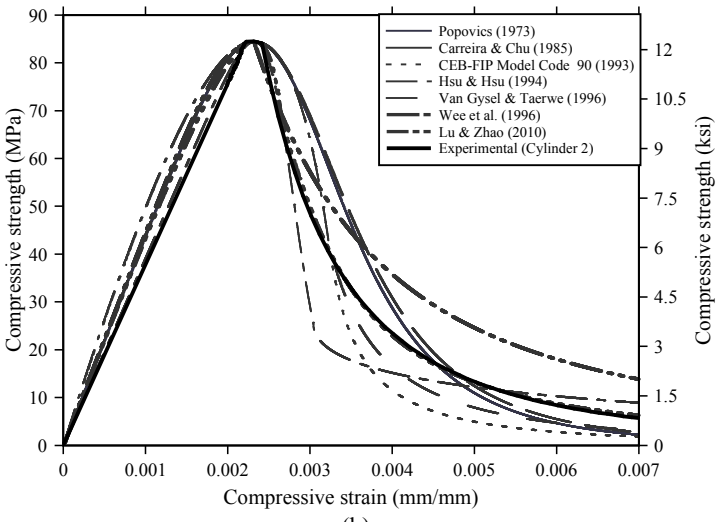

(b)

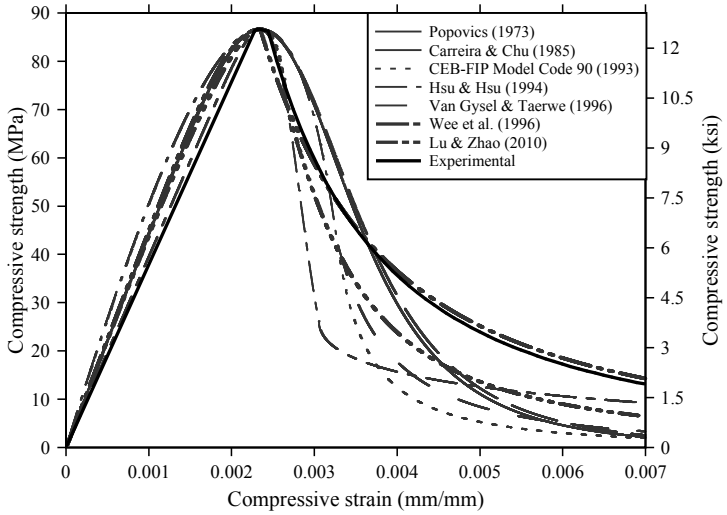

(c)

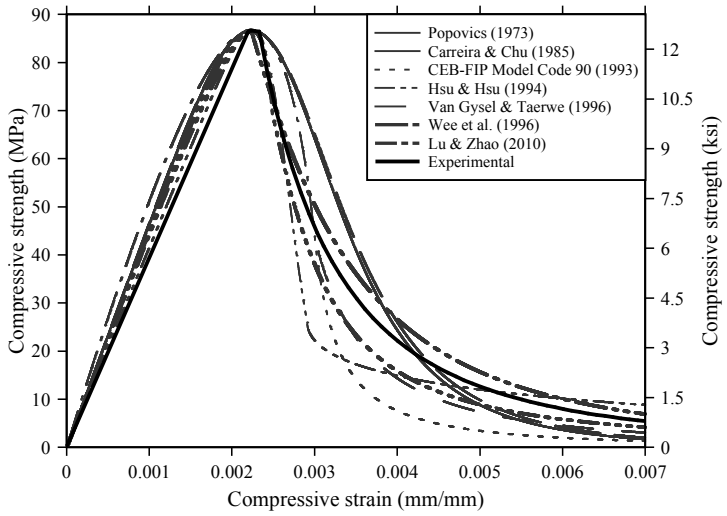

(d)

Fig. 5: Comparison of the predictive and experimental stress-strain curves of series “M"

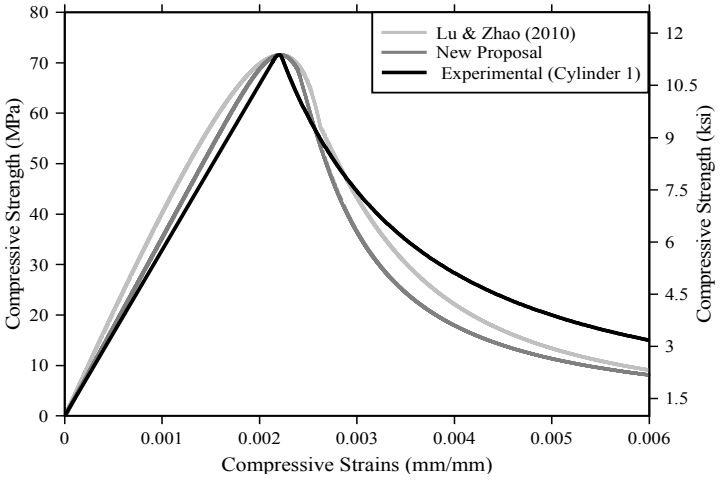

(a)

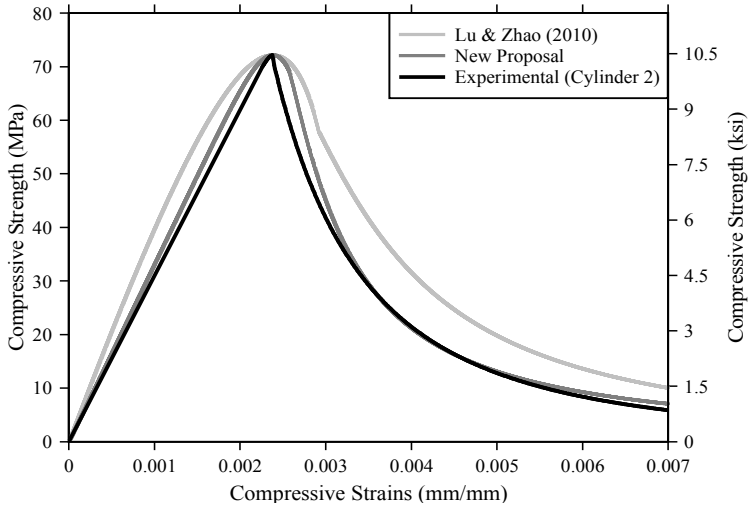

(b)

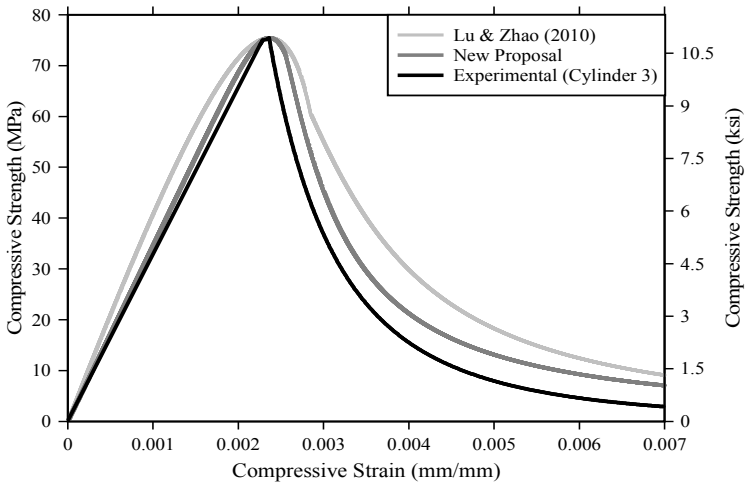

(c)

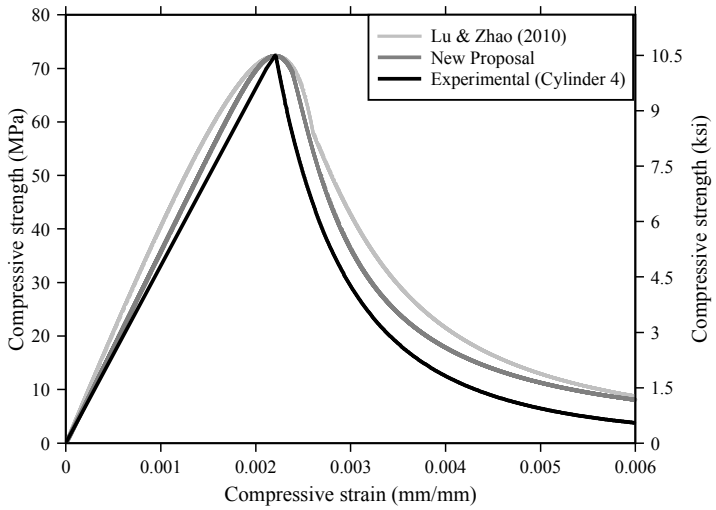

(d)

Fig. 6: Comparison of the proposed model with the experimental data of series "P" and the proposed model of Lu and Zhao (2010)

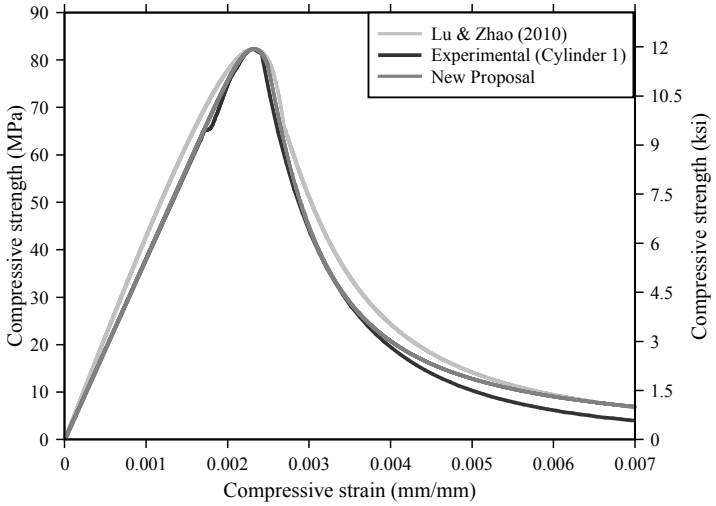
Lu & Zhao (2010)
Experimental (Cylinder 1)
New Proposal
Compressive strength (MPa)
Compressive strength (ksi)
Compressive strain (mm/mm)
0
10
20
30
40
50
60
70
80
90
1.5
3
4.5
6
7.5
9
10.5
12
0.001
0.002
0.003
0.004
0.005
0.006
0.007

(a)

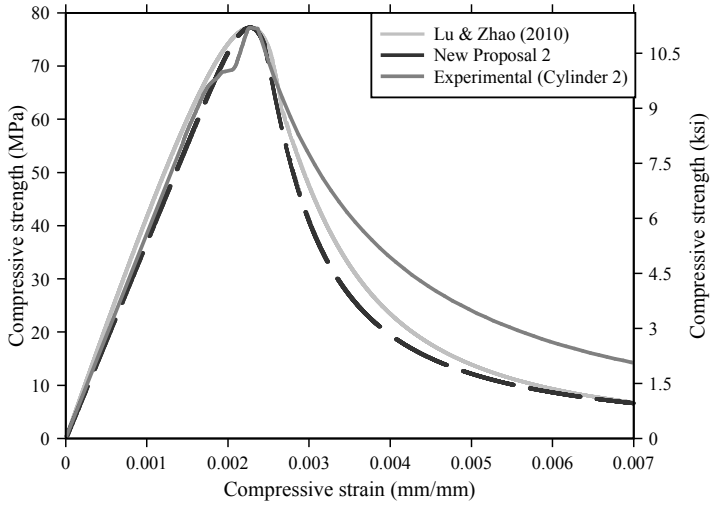
Lu & Zhao (2010)
New Proposal 2
Experimental (Cylinder 2)
Compressive strength (MPa)
Compressive strength (ksi)
Compressive strain (mm/mm)
0
10
20
30
40
50
60
70
80
1.5
3
4.5
6
7.5
9
10.5
0.001
0.002
0.003
0.004
0.005
0.006
0.007

(b)

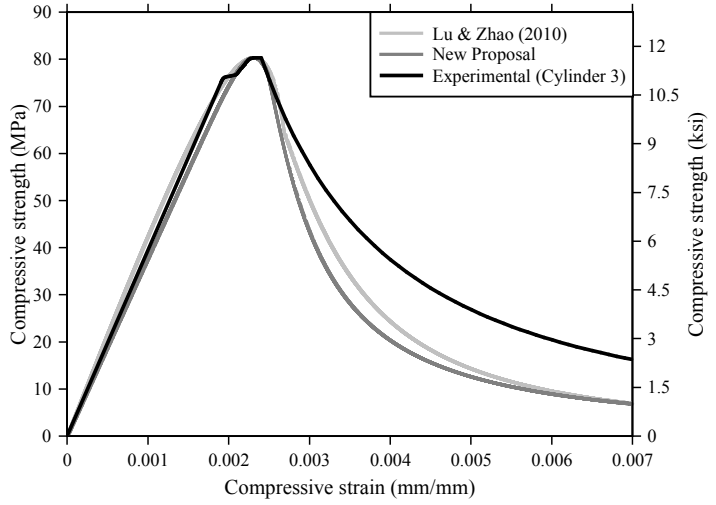
Lu & Zhao (2010)
New Proposal
Experimental (Cylinder 3)
Compressive strength (MPa)
Compressive strength (ksi)
Compressive strain (mm/mm)
0
10
20
30
40
50
60
70
80
90
1.5
3
4.5
6
7.5
9
10.5
12
0.001
0.002
0.003
0.004
0.005
0.006
0.007

(c)

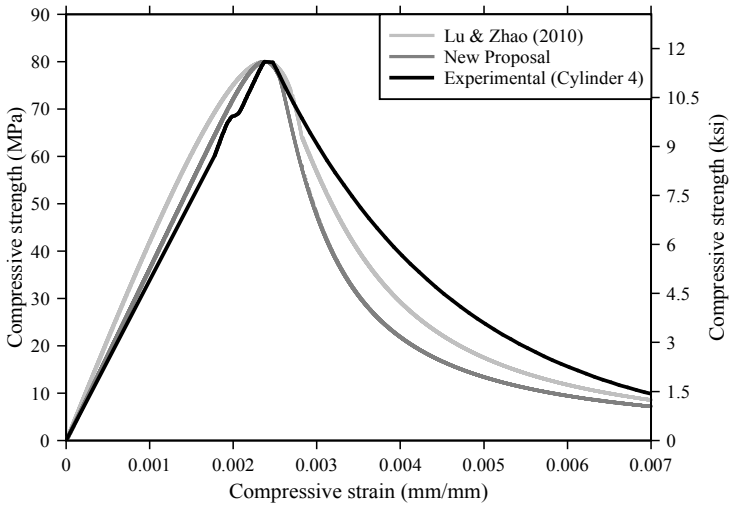

(d)

Fig. 7: Comparison of the proposed model with the experimental data of series "S" and the proposed model of Lu and Zhao (2010)

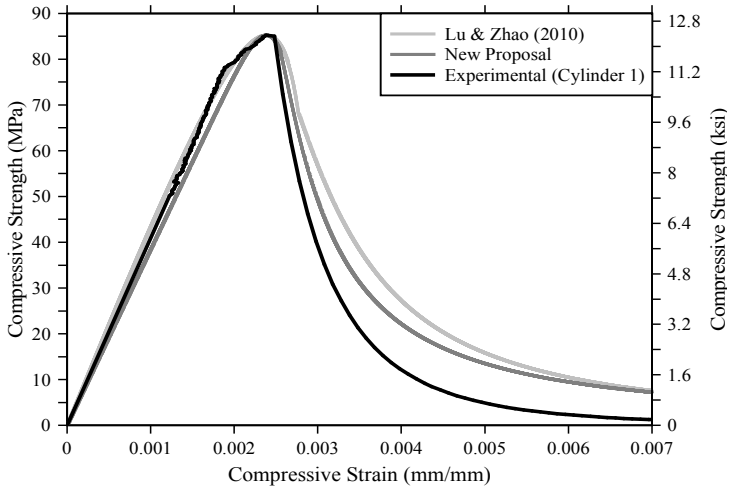

(a)

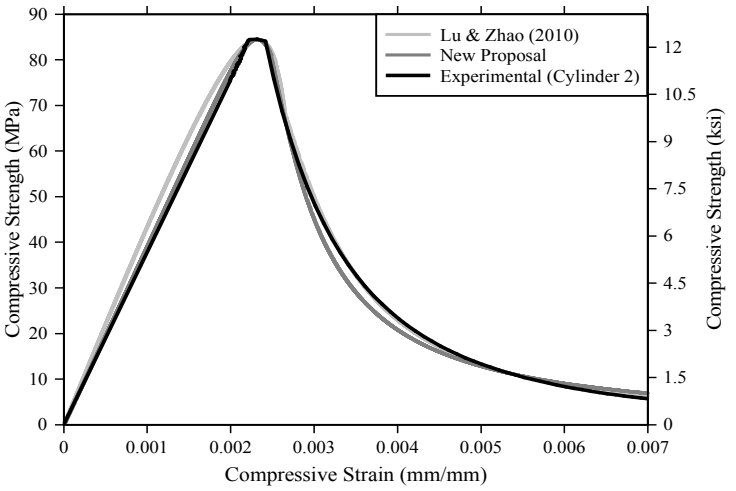

(b)

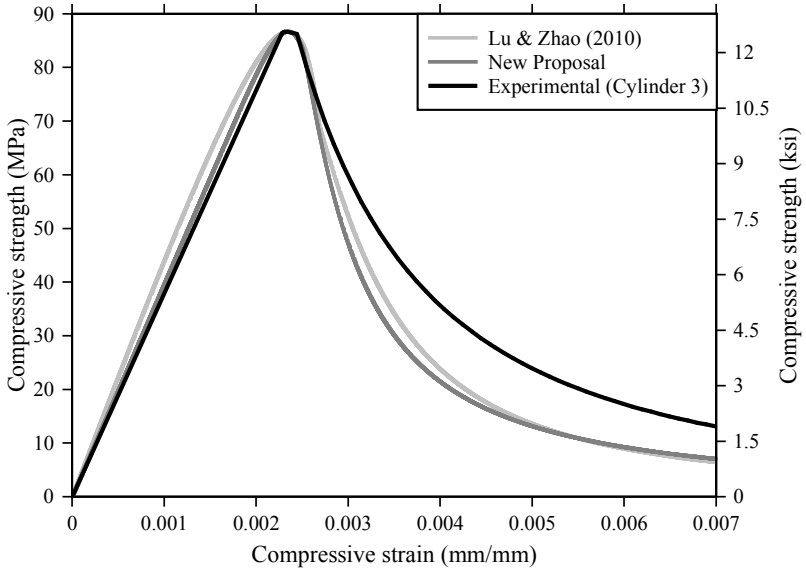

(c)

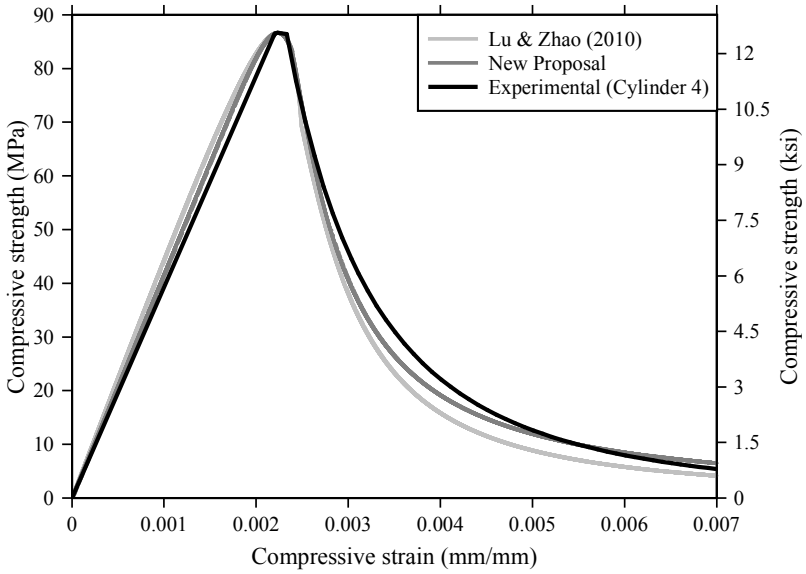

(d)

Fig. 8: Comparison of the proposed model with the experimental data of series "M" and the proposed model of Lu and Zhao (2010)

ascending and descending branches of the stress-strain curves.

Using Eq. (1) and (2), new stress-strain curves are generated and shown in Fig. 6 (for series "P"), Fig. 7 (for Series "S") and Fig. 8 (for Series "M"). In the following figures, the predicted stress-strain curves are also compared with the experimental stress-strain curves and those generated by using the model of Lu and Zhao (2010). It can be observed that, the proposed model for the prediction of stress-strain curves can better predicts the stress-strain curves as compared to the model of Lu and Zhao (2010).

The fit goodness of the predicted stress-strain curves to the experimental stress-strain curves is shown in Table 5, which confirms that the proposed model predicts the stress-strain curves better than the predictive model of Lu and Zhao (2010).

It is worth mentioning that, the predictive model proposed by the authors is investigated for the current mix design (Table 2) and the testing conditions mentioned in this study. In case of different mix design and testing conditions, predictive results and $f_{c,lim}$ may tend to vary (Table 7).

Table 7: Comparison of the "RMS" and "V" values for the proposed predictive model

Series	Cylinder	Parameters	Lu and Zhao (2010)	New proposed model
"P"	Cylinder 1	RMS	3.1110	3.9183
		Variance	0.9492	0.9044
	Cylinder 2	RMS	4.2600	2.2290
		Variance	0.9600	0.9939
	Cylinder 3	RMS	8.9770	4.8516
		Variance	0.8725	0.9500
	Cylinder 4	RMS	7.1000	4.9304
		Variance	0.9132	0.9503
	Series "P"	RMS	5.8620	3.9820
	Average	Variance	0.9237	0.9497
"S"	Cylinder 1	RMS	3.7400	2.6811
		Variance	0.9953	0.9973
	Cylinder 2	RMS	5.0190	5.6251
		Variance	0.9882	0.9834
	Cylinder 3	RMS	6.4780	7.2522
		Variance	0.9618	0.9507
	Cylinder 4	RMS	4.5010	4.3145
		Variance	0.9900	0.9898
	Series "S"	RMS	4.9345	4.9682
	Average	Variance	0.9838	0.9803
"M"	Cylinder 1	RMS	5.7180	5.0944
		Variance	0.9898	0.9908
	Cylinder 2	RMS	1.3670	1.5851
		Variance	0.9988	0.9984
	Cylinder 3	RMS	6.3230	6.9560
		Variance	0.9411	0.9242
	Cylinder 4	RMS	3.1780	1.9685
		Variance	0.9842	0.9944
	Series "M"	RMS	5.1230	4.1470
	Average	Variance	0.9840	0.9785
Average		RMS	4.9810	4.2840
		Variance	0.9620	0.9690

CONCLUSION

The published predictive models are evaluated in this study using the experimental results of two series of HSC including concrete without replacing cement content (i.e., plain concrete) and concrete in which 10% volume of the Meakaolin (MK) was added as a partial replacement of OPC. The experimental results of maximum compressive strength and its corresponding strain were used as input parameters of the proposed predictive models to generate the complete stress-strain curves. The following conclusions can be drawn from this study:

- The stress-strain curves generated by using all existing predictive models do not show good agreement with the current experimental data; however, the predictive model of Hsu and Hsu (1994), as well as that of Lu and Zhao (2010) predict the rising and falling branches of stress-strain curves of HSC, respectively. This was confirmed by comparing the values of the root mean square errors "RMS" and coefficients of variance "V" for all the productive curves with the experimental curves.
- A new predictive model, based on the models of Hsu and Hsu (1994) and Lu and Zhao (2010) is proposed to further refine the stress-strain curves in order to fully utilize the engineering properties of HSC. The predicted stress-strain curves showed good agreement with the experimental results based on the calculations of root mean square errors "RMS" and coefficients of variance "V".

ABBREVIATIONS

Following notations are used in this article:

f_c, ε_c = Coordinates of any stress and strain point on the stress-strain curve of plain concrete

$f_c^{'}$ = Unconfined cylindrical concrete compressive strength of plain concrete

$\varepsilon_c^{'}$ = Strain corresponding to the peak compressive strength of plain concret

E_{it} = Initial tangent modulus of elasticity

E_c = Secant modulus at peak stress ($E_c = fc'\varepsilon c'$ for plain concrete

k, k_1 and k_2 = Correction factors

n, β = Material parameters, β depends on the shape of the stress-strain curves and n depends on the strength material

w = Unit weight of concrete

$\varepsilon_{c,lim}$ = Concrete strain corresponding to particular limit stress on the falling branch of the stress-strain curve

REFERENCES

ASTM, 2003. ASTM C39-03: Standard Test Method for Compressive Strength of Cylindrical Concrete Specimens. ASTM, West Conshohocken, PA, USA.

Carreira, D.J. and K.H. Chu, 1985. Stress-strain relationship for plain concrete in compression. ACI J., 85: 797-804.

CEB-FIP Code 90, 1993. Model Code for Concrete Structures. Bulletin D'Information (117-E). British Standard Institution, London, UK.

Hognestad, E., 1951. Study of combined bending and axial load in reinforced concrete members. Bulletin No. 399, University of Illinois, Engineering Experiment Station.

Hsu, L. and C.T. Hsu, 1994. Complete stress-strain behaviour of high-strength concrete under compression. Mag. Concrete Res., 46(169): 301-312.

Khan, S., T. Ayub and S.F.A. Rafeeqi, 2013. Prediction of compressive strength of plain concrete confined with ferrocement using Artificial Neural Network (ANN) and comparison with existing mathematical models. Am. J. Civil Eng. Archit., 1: 7-14.

Lu, Z.H. and Y.G. Zhao, 2010. Empirical stress-strain model for unconfined high-strength concrete under uniaxial compression. J. Mater. Civil Eng., 22(11): 1181-1186.

Popovics, S., 1973. A numerical approach to the complete stress-strain curve of concrete. Cement Concrete Res., 3(5): 583-599.

Sargin, M. and V. Handa, 1969. A general formulation for the stress-strain properties of concrete. SM Report Solid Mechanics Division, University of Waterloo, Canada, No. 3.

Van Gysel, A. and L. Taerwe, 1996. Analytical formulation of the complete stress-strain curve for high strength concrete. Mater. Struct., 29(9): 529-533.

Wang, P., S. Shah and A. Naaman, 1978. Stress-strain curves of normal and lightweight concrete in compression. ACI J., 75: 603-611.

Wee, T., M. Chin and M. Mansur, 1996. Stress-strain relationship of high-strength concrete in compression. J. Mater. Civil Eng., 8(2): 70-76.